AMERICAN SOCIETY FOR MICROBIOLOGY | Antimicrobial Agents and Chemotherapy®

Molecular Bases Determining Daptomycin Resistance-Mediated Resensitization to β-Lactams (Seesaw Effect) in Methicillin-Resistant *Staphylococcus aureus*

Adriana Renzoni,[a] William L. Kelley,[b] Roberto R. Rosato,[c] Maria P. Martinez,[c] Melanie Roch,[c] Maryam Fatouraei,[c] Daniel P. Haeusser,[d] William Margolin,[d] Samuel Fenn,[e] Robert D. Turner,[e] Simon J. Foster,[e] Adriana E. Rosato[c]

Hopitaux Universitaires de Genève, Service of Infectious Diseases, Geneva, Switzerland[a]; University of Geneva Medical School, Department of Microbiology and Molecular Medicine, Geneva, Switzerland[b]; Department of Pathology and Genomic Medicine, Center for Molecular and Translational Human Infectious Diseases Research, Houston Methodist Research Institute, Houston, Texas, USA[c]; Department of Microbiology and Molecular Genetics, McGovern Medical School, University of Texas, Houston, Texas, USA[d]; Krebs Institute, University of Sheffield, Sheffield, United Kingdom[e]

ABSTRACT Antimicrobial resistance is recognized as one of the principal threats to public health worldwide, yet the problem is increasing. Infections caused by methicillin-resistant *Staphylococcus aureus* (MRSA) strains are among the most difficult to treat in clinical settings due to the resistance of MRSA to nearly all available antibiotics. The cyclic anionic lipopeptide antibiotic daptomycin (DAP) is the clinical mainstay of anti-MRSA therapy. The decreased susceptibility to DAP (DAP resistance [DAP^r]) reported in MRSA is frequently accompanied by a paradoxical decrease in β-lactam resistance, a process known as the "seesaw effect." Despite the observed discordance in resistance phenotypes, the combination of DAP and β-lactams has been proven to be clinically effective for the prevention and treatment of infections due to DAP^r MRSA strains. However, the mechanisms underlying the interactions between DAP and β-lactams are largely unknown. In the study described here, we studied the role of *mprF* with DAP-induced mutations in β-lactam sensitization and its involvement in the effective killing by the DAP-oxacillin (OXA) combination. DAP-OXA-mediated effects resulted in cell wall perturbations, including changes in peptidoglycan insertion, penicillin-binding protein 2 (PBP 2) delocalization, and reduced membrane amounts of PBP 2a, despite the increased transcription of *mecA* through *mec* regulatory elements. We have found that the VraSR sensor-regulator is a key component of DAP resistance, triggering mutated *mprF*-mediated cell membrane (CM) modifications that result in impairment of PrsA location and chaperone functions, both of which are essential for PBP 2a maturation, the key determinant of β-lactam resistance. These observations provide for the first time evidence that synergistic effects between DAP and β-lactams involve PrsA posttranscriptional regulation of CM-associated PBP 2a.

KEYWORDS MRSA, daptomycin, seesaw effect, β-lactams, PrsA, β-lactams

Received 27 July 2016 **Returned for modification** 1 September 2016 **Accepted** 12 October 2016

Accepted manuscript posted online 24 October 2016

Citation Renzoni A, Kelley WL, Rosato RR, Martinez MP, Roch M, Fatouraei M, Haeusser DP, Margolin W, Fenn S, Turner RD, Foster SJ, Rosato AE. 2017. Molecular bases determining daptomycin resistance-mediated resensitization to β-lactams (seesaw effect) in methicillin-resistant *Staphylococcus aureus*. Antimicrob Agents Chemother 61:e01634-16. https://doi.org/10.1128/AAC.01634-16.

Address correspondence to Adriana E. Rosato, aerosato@HoustonMethodist.org.

Staphylococcus aureus has a proclivity for developing multidrug resistance (e.g., methicillin-resistant *S. aureus* [MRSA]), and infections with this pathogen result in enhanced attributable mortality (1). Since its FDA approval in 2003, the cyclic anionic lipopeptide antibiotic daptomycin (DAP), produced by *Streptomyces roseosporus* (2), has become the clinical mainstay of anti-MRSA therapy due to its potent staphylocidal

activity (3). The mechanism of action of DAP involves the disruption of the cytoplasmic membrane (CM) function, leading to its depolarization and causing cell death (4). However, there have been a number of reports in which initially DAP-susceptible (DAP^s) MRSA strains developed DAP-resistant (DAP^r) phenotypes during clinical treatment failures (5, 6). DAP^r strains obtained from patients with therapeutic failure have a number of gene mutations linked with DAP resistance, including mutations in genes associated with the CM (e.g., *mprF*) and the cell wall (CW) (e.g., the two-component system YycFG), as well as other mutations, such as mutations in RNA polymerase subunits RpoB and RpoC (7). However, the most clinically significant and relevant changes are those associated with mutations in *mprF* (5, 6). In previous studies, we demonstrated by using sets of isogenic DAP^s and DAP^r strains that, in addition to *mprF*, resistance to DAP involves the upregulation of genes involved in CW synthesis and turnover, including the two-component regulator and CW stress stimulon *vraSR* (6). Together, these observations led us to postulate that both CM and CW components contribute to decreased susceptibility to DAP.

Interestingly, we and others have observed both *in vitro* (8–10) and *in vivo* (8, 11, 12) that DAP resistance sensitizes MRSA to β-lactams, notably, oxacillin (OXA), a process known as a "seesaw effect" (8). Indeed, we have demonstrated that combinations of DAP with OXA (*in vitro*) or nafcillin (NAF) (*in vivo*), as well as other β-lactams, such as cefotaxime (CTX), which targets penicillin-binding protein 2 (PBP 2), and carbapenems, such as imipenem (IPM), that target PBP 1, displayed strong synergistic interactions resulting in activity against DAP-resistant MRSA isolates (8). Although the DAP–β-lactam combination is extensively used in clinical settings for the treatment of MRSA infections associated with decreased susceptibility to DAP (8), the mechanistic bases of the seesaw effect remain to be elucidated.

The PrsA protein is required for resistance to oxacillin as well as glycopeptide antibiotics in *S. aureus* (13, 14). In Gram-positive bacteria, such as *Bacillus subtilis* and *Listeria monocytogenes*, PrsA is a membrane-anchored protein that catalyzes the post-translocational folding of exported proteins and is essential for their stability as they cross the bacterial cell membrane-cell wall interface (15, 16). In *B. subtilis*, PrsA is required for the folding of penicillin-binding proteins (PBPs) and lateral cell wall biosynthesis; in the absence of PrsA, four PBPs (PBP 2a, PBP 2b, PBP 3, and PBP 4) become unstable (17). Additionally, in *L. monocytogenes*, PrsA2 contributes to bacterial pathogenesis and virulence (18). Expression of *prsA* is induced when it encounters cell wall-active antibiotics, and induction is dependent upon the activity of VraSR, the cell wall stress two-component system (14). Importantly, the same authors reported that cells were more susceptible to oxacillin in the absence of PrsA, suggesting that PrsA may be involved in oxacillin resistance in concert with VraSR, PBP 2, and PBP 2a (14). Recent PrsA structure and function analyses revealed that PrsA modulates PBP 2a protein levels independently of the staphylococcal cassette chromosome *mec* element (SCC*mec*) background of the strains (13). Regulation of PBP 2a expression at the transcriptional level involves *mecI*, *mecR*, and *blaRZ*, which may vary in different SCC*mec* types, but less is known about the posttranscriptional maturation and proper localization of PBP 2a.

In the present study, we demonstrate that DAP^r-mediated *mprF* mutations result in significant changes in cell wall synthesis by influencing the function of PrsA, which correlates with reduced amounts of β-lactam-induced PBP 2a. This work provides evidence that MprF and PrsA are important for the sensitization to β-lactams during DAP resistance in MRSA (the seesaw effect) and contributes new insights into the mechanisms associated with this effect.

RESULTS

Daptomycin-induced cytoplasmic membrane and cell wall changes. Despite considerable evidence pointing to the action of DAP on the CM, the CW has also been suspected to be an important target, as recently shown in *B. subtilis* (19, 20). We used fluorescence microscopy to visualize the effects of DAP on both CM and CW functions.

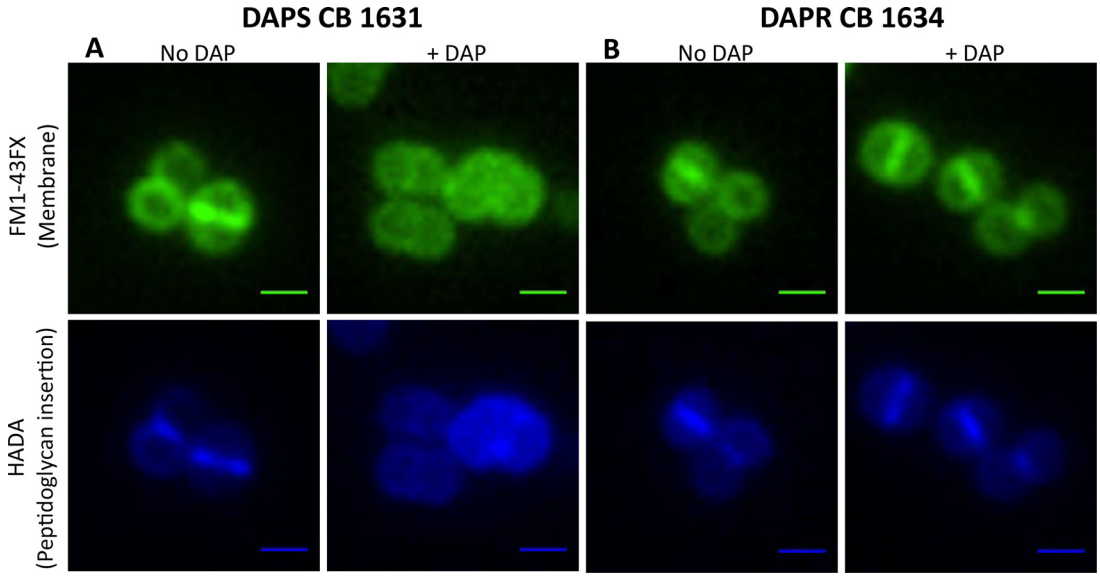

FIG 1 Effects of DAP on the cytoplasmic membrane and cell wall of the DAP^s CB1631 (A) or DAP^r CB1634 (B) bacterial strain. Bacteria were grown in TSB (with or without DAP) at 37°C to late exponential phase (2.5 h) and labeled for 5 min with FM1-43FX (membrane; top) or HADA (peptidoglycan insertion; bottom). A Nikon inverted epifluorescence microscope was used. Exposure and contrast settings were optimized for each image; i.e., the brightness was not comparable between fields. Scale bars are 1 μm.

When DAP^s CB1631 cells were treated with DAP, they displayed significant morphological changes at the CM level (Fig. 1A, FM1-43FX staining, top), including shape abnormalities and size heterogeneity compared with the shapes and sizes of untreated control cells (Fig. 1A, No DAP). All the cells contained DNA, as judged by DAPI (4′,6-diamidino-2-phenylindole) staining (not shown), indicating that DAP did not cause significant alterations to the nucleoid.

This observation was corroborated by analysis of the pattern of nascent peptidoglycan insertion using the fluorescent D-amino acid derivative 7-hydroxycoumarin 3-carboxylic acid (HCC)-3-amino-D-alanine (HADA). Exposure of DAP^s CB1631 to DAP induced the delocalization of peptidoglycan insertion (Fig. 1A, bottom), suggesting that PBPs were displaced from the division septum, where CW synthesis normally takes place. Importantly, none of the changes described in DAP^s CB1631 were observed in the DAP^r CB1634 counterpart (Fig. 1B, right). These observations are in agreement with the hypothesis that DAP induces dramatic effects on both the CM and CW in *S. aureus*.

Effects on cell wall rearrangements during exposure to a combination of DAP and β-lactams. We previously observed that DAP-mediated sensitization to β-lactams occurred with those β-lactams that preferentially target PBP 1 or PBP 2, including NAF (PBP 1, PBP 2), IPM (PBP 1), and CTX (PBP 2), whereas no changes were observed with β-lactams targeting PBP 4, such as cefoxitin (FOX), or PBP 3, such as cefaclor (CEC) (8, 21, 22). Similar effects were observed in other *in vitro*-selected DAP^r mutants obtained from DAP^s CB1631 (DAP^r CB1631 mutants) and CB5011 (DAP^r CB5011 mutants) (8). Collectively, these observations suggest that the seesaw effect involves CW modifications.

To address this in more detail, we stained cells with Bodipy FL-vancomycin (VAN), which has been used extensively to detect the localization of newly synthesized peptidoglycan in Gram-positive bacteria (23, 24). DAP^r CB1634 cells were grown without or with the DAP-OXA combination and then stained with Bodipy FL-VAN (10 min) for detection of peptidoglycan by fluorescence microscopy (Fig. 2). In the untreated control, Bodipy FL-VAN intensely stained the complete equatorial cell septa and faintly stained the side walls; in contrast, cells grown in the presence of DAP-OXA showed mostly delocalized Bodipy FL-VAN staining (Fig. 2A). These results are consistent with the delocalized peptidoglycan insertion patterns observed by HADA staining (Fig. 1) and suggest that the coadministration of DAP with β-lactams causes dramatic

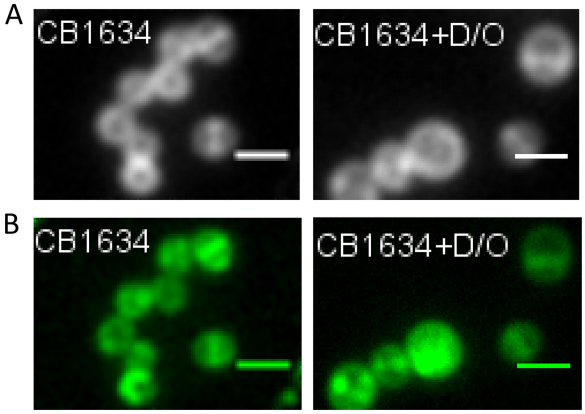

FIG 2 Localization of PBP 2-GFP fusions in DAP^r cells treated with OXA, DAP, or DAP-OXA. (A) The DAP^r CB1634 strain producing PBP 2-GFP was grown with or without sublethal concentrations of DAP-OXA (D/O; 0.5× MIC), followed by labeling with Bodipy FL-VAN, fixation, and imaging by fluorescence microscopy. (B) DAP^r CB1634 cells producing PBP 2-GFP were induced with IPTG in the presence or absence of DAP, OXA, or the DAP-OXA combination, fixed, and imaged by fluorescence microscopy. Scale bars are 1 μm.

local effects on the CW in DAP^r cells similar to those observed in DAP^s cells (CB1631), such as displacement of PBPs from the septum. In fact, studies of the labeling of newly synthesized CW with fluorescein-conjugated VAN in *S. aureus* have suggested that most CW synthesis is confined to the division septum, where both PBP 1 and PBP 2 are localized (25).

To investigate further the hypothesis that the combined effects of DAP and β-lactams on the CW contribute to the delocalization of PBPs, particularly PBP 1 and PBP 2, we generated a CB1634 derivative strain expressing an IPTG (isopropyl-β-D-thiogalactopyranoside)-regulated PBP 2-green fluorescent protein (GFP) fusion protein. Analysis of untreated cells of the CB1634 strain expressing PBP 2-GFP showed that the PBP 2-GFP protein clearly localized to the equatorial cell septa (Fig. 2B). In contrast, exposure to the DAP-OXA combination resulted in a diffused and delocalized distribution of PBP 2-GFP, in agreement with the results in Fig. 2A. Similar observations were made by using the same approach with a PBP 1-GFP fusion protein (data not shown). We next wanted to determine the activity of PBPs by measuring their affinity of binding to a fluorescent β-lactam, Bocillin FL. The DAP^r CB1634 strain was exposed to DAP (1 μg/ml), OXA (0.5 μg/ml), and DAP-OXA (1 μg/ml and 0.5 μg/ml, respectively), and PBPs, separated by sodium dodecyl sulfate (SDS)-PAGE, were analyzed for their ability to bind Bocillin FL. As shown in Fig. 3, DAP^r CB1634 cells treated with DAP-OXA and subsequently labeled with Bocillin FL displayed decreased levels of PBP 1, PBP 2, and PBP 3, whereas no changes were observed with either DAP or OXA alone or both DAP and OXA. However, since we have previously shown that inhibition of PBP 3 by CEC did not result in a seesaw effect when CEC was combined with DAP (8), the present results may indicate that PBP 1 and PBP 2 have a relevant role in the DAP-associated seesaw effect and restoration of susceptibility to β-lactams in DAP^r MRSA strains.

Sensitization to β-lactams during DAP resistance is associated with decreased production of PBP 2a. β-Lactam resistance in MRSA involves the horizontal acquisition of the *mecA* gene, which encodes PBP 2a, a PBP with a low affinity for β-lactams that can mediate cell wall assembly when the normal staphylococcal PBPs (PBPs 1 to 4) are inactivated by these agents (25). To determine a potential role for PBP 2a in the DAP-mediated seesaw effect observed in the DAP^r strains, PBP 2a protein expression levels were analyzed by Western blotting using cell membrane protein extracts prepared from CB1634 cells treated with OXA, DAP, and the DAP-OXA combination. PBP 2a induction was observed in untreated control cells, but no PBP 2a induction was observed after DAP treatment, while, as expected, the levels of PBP 2a increased significantly after exposure to OXA (Fig. 4A). Importantly, in DAP-OXA-treated CB1634

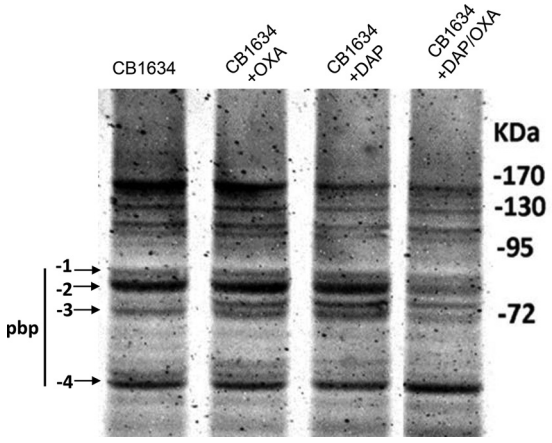

FIG 3 Analysis of PBPs from CB1634 cells treated with OXA, DAP, or DAP-OXA. Membrane preparations obtained from CB1634 cells untreated or treated with OXA (0.5 μg/ml), DAP (1 μg/ml), or DAP-OXA (0.5 μg/ml and 1 μg/ml, respectively) were analyzed for the detection of penicillin-binding proteins 1 to 4. Equal amounts (20 μg) of Bocillin FL-labeled membrane proteins were separated by 10% SDS-PAGE. Arrows, fluorescently labeled PBPs.

cells, there was a marked reduction in PBP 2a levels compared to those after OXA induction. Analysis of extracellular extracts normalized to their optical density at 600 nm (OD_{600}) showed increased amounts of extracellular PBP 2a in extracts from the CB1634 strain treated with DAP-OXA, while no extracellular PBP 2a was detected in extracts from the untreated control sample (Fig. 4A). A slight increase in the extracellular amounts of PBP 2a was also observed in extracts from OXA-treated cells, consistent with increasing amounts of cell membrane-associated protein. These results strongly suggest that PBP 2a localization to the CM is altered, which in turn would be associated with the DAP^r phenotype-mediated seesaw effect.

To determine whether the reduction of PBP 2a levels observed with the DAP-OXA combination was linked to alterations in *mecA* transcriptional regulation, we evaluated *mecA* mRNA levels in the absence and presence of DAP, OXA, and DAP-OXA by real-time reverse transcription-PCR (RT-PCR) analysis. We found that *mecA* transcription in the CB1634 strain displayed significant induction by OXA alone, an effect that was further enhanced in the case of induction by the combination OXA-DAP (Fig. 4B); a modest induction was also observed upon exposure to DAP. These results do not correlate with the changes in the levels of the CM-associated PBP 2a protein after treatment with the various drug combinations and thus cannot be attributed solely to changes in the level of transcription of the *mecA* gene. Furthermore, the results strongly suggest that these alterations during the seesaw effect may critically interfere with the normal synthesis/function of the CW.

We next wanted to establish whether DAP-induced mutations in *mprF*, which are potentially associated with changes in the CM, may play a role in PBP 2a and the changes to the CW observed during the seesaw effect. To address this, we analyzed PBP 2a protein levels using membrane protein extracts from DAP^r CB1634, CB1634 Δ*mprF*, and CB1634 Δ*mprF* complemented with either wild-type (WT) *mprF* or a previously isolated *mprF* mutant with an L-to-F amino acid change at position 826 (*mprFL826F*) that is associated with decreased susceptibility to DAP (6). As depicted in Fig. 4C, the cellular levels of membrane-associated PBP 2a were sharply increased by exposure to OXA in all strains compared to the levels in either the corresponding untreated controls or DAP-treated cells. Importantly, the strong reduction of PBP 2a levels in the parental CB1634 strain exposed to DAP-OXA (Fig. 4A) was not observed in the CB1634 Δ*mprF* strain, strain MAR17 (Fig. 4C). Interestingly, complementation of MAR17 with WT *mprF* (strain MAR18) resulted in the same PBP 2a profile detected in MAR17, indicating that there were no differences in the amount of CM-associated protein between OXA- and DAP-OXA-treated cells. However, PBP 2a levels were significantly reduced in CB1634

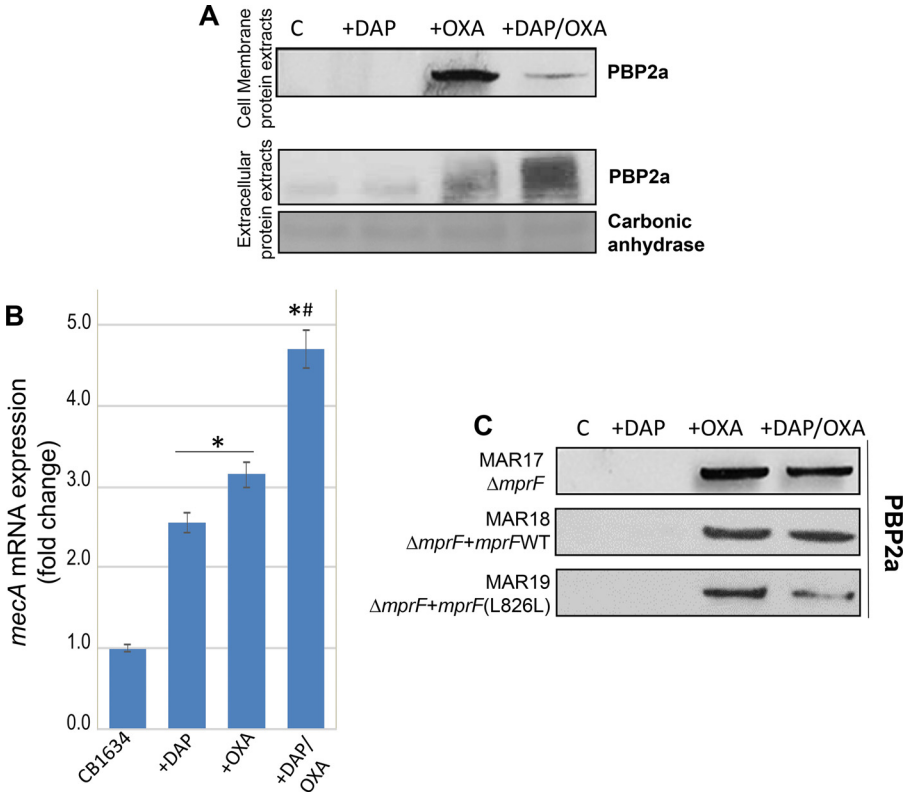

FIG 4 Sensitization to β-lactams during DAP resistance is associated with decreased production of PBP 2a. (A) Western blot analysis of the PBP 2a protein in membrane and extracellular protein extracts from DAP^r CB1634 cells grown without (control [C]) or with DAP, OXA, or the DAP-OXA combination. Carbonic anhydrase was used as a loading control. (B) RT-PCR analysis showing *mecA* gene expression in DAP^r CB1634 cells grown without or with DAP, OXA, or the DAP-OXA combination. *, the fold change was significantly higher than that for the CB1634 control (no antibiotic) ($P < 0.05$); #, the fold change was significantly higher than that for cells exposed to DAP or OXA alone ($P < 0.05$). (C) Western blot analysis of the PBP 2a protein in membrane protein extracts from CB1643 Δ*mprF* (MAR17), CB1634 Δ*mprF mprF* (WT) (MAR18), and CB1634 Δ*mprF mprFL826F* (MAR19) cells grown without (control) or with DAP, OXA, or the DAP-OXA combination.

Δ*mprF* complemented with *mprFL826F* (strain MAR19), following the same pattern observed in the parental CB1634 strain displaying the seesaw effect. These results indicate that the DAP-mediated changes in *mprF* and/or the CM associated with the DAP^r phenotype alter the membrane levels of PBP 2a and thereby may interfere with the normal synthesis/function of the CW.

Functional role of *mprF* mutations on peptidoglycan cross-linking and DAP availability during DAP^r and the seesaw effect. Given the effects of altered MprF on PBP 2a levels, we next wanted to determine the influence of *mprF* mutations on the DAP-mediated seesaw effect. Phenotypic analysis comparing DAP^r CB1634 and its CB1634 Δ*mprF* counterpart showed that inactivation of *mprF* led to increased susceptibility to DAP (DAP MICs, 4 μl/ml and 0.25 μl/ml, respectively) and increased resistance to OXA (OXA MICs, 0.5 μl/ml and 32 μl/ml, respectively) (Table 1). Importantly,

TABLE 1 MICs of DAP and OXA for DAP^r CB1634 and *mprF* derivatives determined by Etest

Strain	MIC (μg/ml)	
	DAP	OXA
CB1634	4	0.5
CB1634 Δ*mprF*	0.25	32
CB1634 Δ*mprF mprF* (WT)	0.75	32
CB1634 Δ*mprF mprFL826F*	3	1

complementation of CB1634 Δ*mprF* with WT *mprF* did not revert the phenotype (DAP and OXA MICs, 0.75 μg/ml and 32 μg/ml, respectively). In contrast, complementation with *mprFL826F* restored the resistance to DAP (MIC, 3 μg/ml) and decreased the level of resistance to OXA (MIC, 1 μg/ml), reestablishing the DAP-mediated seesaw effect (Table 1). Similar results were observed with the DAP^s-DAP^r pair CB5011 and CB5012 *mprFL826F* (data not shown).

We next determined the impact of *mprF* mutations and the implications of altered levels of PBP 2a on the CW during the DAP-mediated seesaw effect. The muropeptide composition of peptidoglycan was measured in DAP^r CB1634 cells untreated and treated with DAP-OXA after separation by reverse-phase high-performance liquid chromatography (HPLC). Analysis of the HPLC profiles revealed marked differences in CW cross-linking in CB1634 cells with or without DAP-OXA treatment (Fig. 5A), showing that exposure to DAP-OXA resulted in a significant decrease in the amount of highly cross-linked oligomer muropeptides (peaks 17 to 22), which should reduce the rigidity of the CW. These results are in accordance with our data showing that exposure of DAP^r strains to DAP-OXA reduces the levels of PBP 2a associated with the CM, which in turn could lead to the observed CW rearrangements and increased oxacillin susceptibility.

To investigate the role of *mprF* in the CW composition, notably taking into account the observations described above, we compared the muropeptide profiles of CB1634 with those of the CB1634 Δ*mprF* mutant. While no differences in the profiles between the two strains were observed in the absence of antibiotics (Fig. 5B, top), the addition of OXA showed significant enrichment of monomeric and dimeric components in the CB1634 Δ*mprF* strain (Fig. 5B, middle). These *mprF*-dependent effects were further enhanced by coexposure to DAP and OXA (Fig. 5B, bottom), providing a plausible explanation for the ability of the *mprF* deletion in DAP^r strains to reverse the increased susceptibility to OXA during the seesaw effect, as shown in Table 1.

Cross talk between MprF and PrsA proteins. To understand further the molecular mechanism linking the *mprFL826F* mutation with decreased PBP 2a levels in the CM and peptidoglycan cross-linking during the seesaw effect, three basic observations were important to consider. First, we recently demonstrated that PrsA, a lipoprotein acting as a posttranslocational chaperone, is involved in β-lactam resistance by affecting the amounts of PBP 2a in the CM (26); in addition, *prsA* expression is regulated by the two-component system VraSR (14). Second, we have shown that acquisition of DAP^r involves the upregulation of genes controlling CW synthesis and turnover, including *vraSR* (6). Unpublished transcriptome RNA sequencing (RNA-Seq) results suggest that the *vraSR* and *prsA* genes in the DAP^r CB1634 strain are upregulated compared to their level of regulation in the DAP^s CB1631 strain, suggesting a link between the *mprFL826F* mutation present in CB1634 and changes in the expression of both the *vraSR* and *prsA* genes. Third, MprF has been shown to be involved in the modification of the membrane phospholipid phosphatidylglycerol, which in turn acts as a substrate for the Lgt enzyme that modifies lipoproteins, such as PrsA (27).

In light of these observations, we hypothesized that DAP^r-associated *mprF* mutations could affect the ability of PrsA to associate with the CM and, consequently, affect its functional activity. To test whether PrsA and MprF are mutually interconnected during the DAP^r-mediated seesaw effect, we first evaluated the cellular levels of PrsA and the localization of PrsA in both the CM and extracellular protein extracts (Fig. 6). Consistent with the results of RNA-Seq analysis, we observed that steady-state levels of PrsA in the CM were higher in CB1634 than CB1631 (Fig. 6A). Interestingly, the levels of PrsA, which was almost undetectable in the absence of *mprF* (CB1634 Δ*mprF*), were restored by complementation with *mprFL826F* (CB1634 Δ*mprF mprFL826F*) but not with WT *mprF* (CB1634 Δ*mprF mprF*) (Fig. 6A). Concomitant analysis of extracellular extracts for which the OD_{600} was normalized showed increased amounts of extracellular PrsA in the corresponding CB1634 Δ*mprF* and CB1634 Δ*mprF mprF* (WT) strains, while no extracellular PrsA was detected in extracts from the CB1634 Δ*mprF mprFL826F* strain

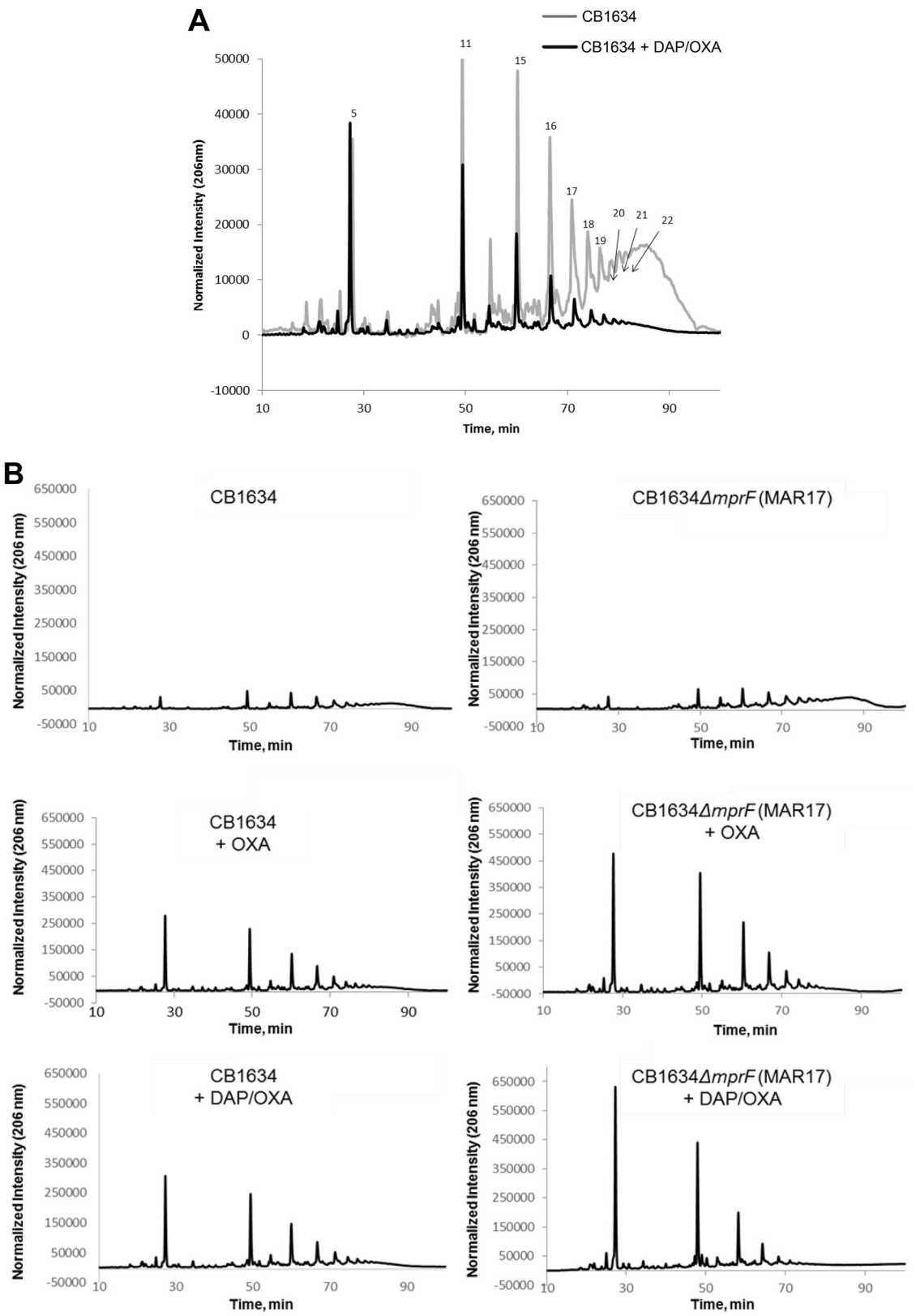

FIG 5 (A) Effect of the DAP-OXA combination on peptidoglycan cross-linking. The peptidoglycan muropeptide composition of DAP^r CB1634 strains grown without or with the DAP-OXA combination was analyzed by reverse-phase HPLC. Peaks numbered 17 to 22 denote highly cross-linked oligomer muropeptides. (B) Effect of *mprF* deletion on peptidoglycan cross-linking in the presence of OXA or the DAP-OXA combination. The peptidoglycan muropeptide composition of DAP^r CB1634 (left) and DAP^s CB1634 Δ*mprF* (right) strains grown without or with OXA or the DAP-OXA combination was analyzed by reverse-phase HPLC.

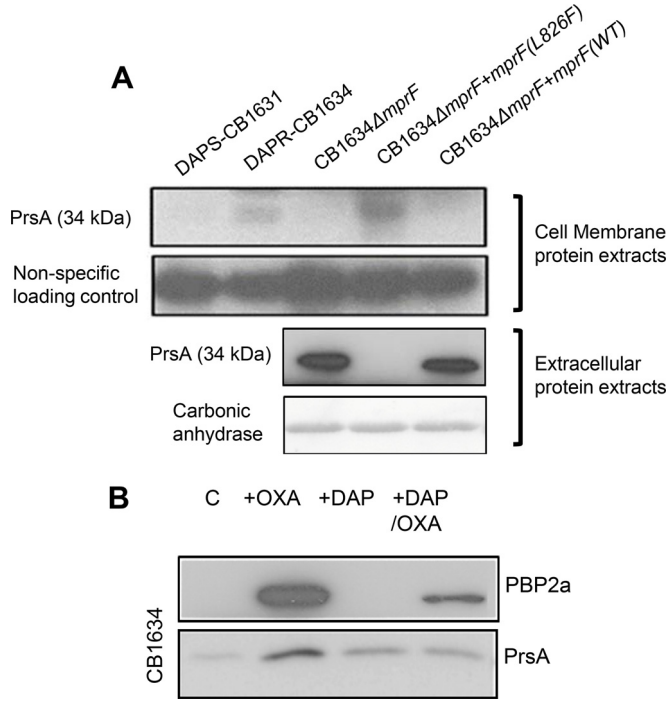

FIG 6 Effect of *mprF* mutations on PrsA membrane localization. (A) Western blot analysis of the PrsA protein in membrane protein extracts (top) and extracellular protein extracts (bottom) from DAP^s CB1631, DAP^r CB1634, CB1643 Δ*mprF*, CB1634 Δ*mprF mprF* (WT), and CB1634 Δ*mprF mprFL826F* cells grown without antibiotics. Carbonic anhydrase was used a loading control. (B) Western blot analysis for PBP 2a and PrsA in membrane extracts from DAP^r CB1634 cells grown without (control [C]) or with OXA, DAP, or the DAP-OXA combination.

(Fig. 6A). These results strongly suggest that PrsA localization to the CM is altered by the *mprF* mutation and that this in turn is associated with the DAP^r phenotype.

PrsA-mediated effects on CM-associated PBP 2a are triggered by the *mprFL826F* mutation. Since DAP-mediated effects during the seesaw effect involve alterations in PBP 2a levels in the membrane (Fig. 4A) and taking into account the PrsA-mediated regulatory role in β-lactam resistance via modulation of PBP 2a (13), we hypothesized that during the acquisition of DAP^r, cell membrane modifications triggered by mutations in *mprF* alter PrsA membrane localization and, consequently, PBP 2a membrane levels. To test this idea, we measured PBP 2a and PrsA protein levels in CM extracts prepared from CB1634 (carrying *mprFL826F*) grown in the absence or presence of DAP, OXA, and the DAP-OXA combination. As shown in the Western blot in Fig. 6B, PBP 2a and PrsA protein membrane levels were increased upon OXA stress, but consistent with our hypothesis, the DAP-OXA combination resulted in decreased cell membrane levels of PBP 2a that correlated with a concomitant reduction in the levels of PrsA. Taken together, our results strongly suggest that despite the DAP-OXA-induced transcriptional upregulation of *mecA*, the *mprF*-dependent loss of CM-anchored PrsA results in the depletion of PBP 2a. Thus, the acquisition of DAP^r via an *mprF*-dependent mechanism results in levels of PBP 2a insufficient to sustain resistance to β-lactams, an effect mediated by the altered cell membrane localization of PrsA.

Homogeneous DAP^r MRSA strains do not display the seesaw effect without DAP induction. In previous studies, we reported that two DAP^r strains, CB5036 and CB5014, with mutations in the central domain of MprF, P314L and S377L, respectively, did not display the DAP-mediated seesaw effect; i.e., their OXA MICs remained the same (512 μg/ml) in both strains of pairs of DAP^s-DAP^r strains (strains CB5035 [DAP^s] and CB5036[DAP^r] and strains CB5013 [DAP^s] and CB5014[DAP^r]) (8). However, as we described previously, the DAP-OXA combination was still effective against them (8). These strains are called homogeneous MRSA because they express a uniformly high

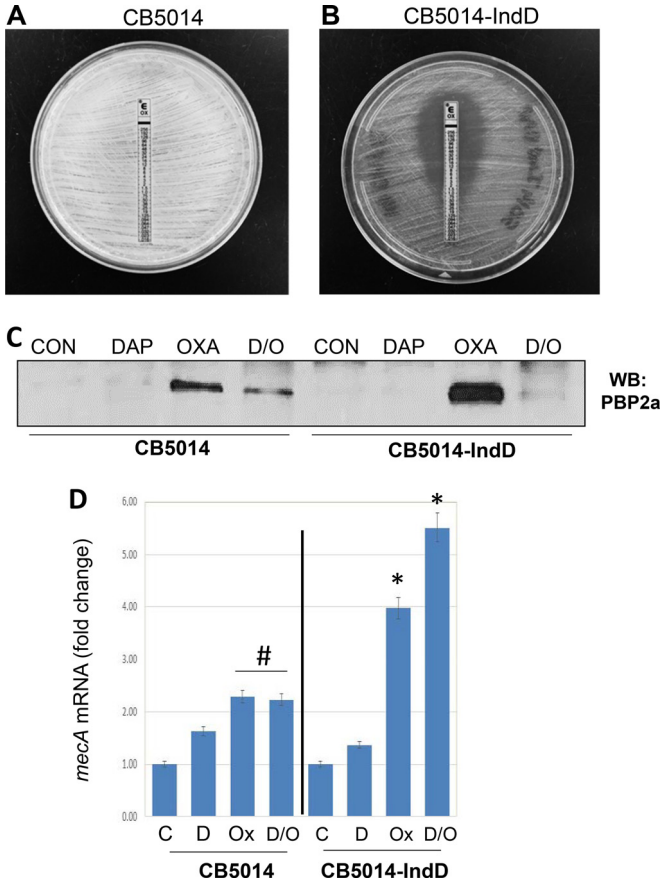

FIG 7 Homogeneous DAP^r MRSA strains do not display the seesaw effect without DAP induction. DAP^r strain CB5014 grown overnight in the absence (A) and in the presence (B) (strain CB5014IndD) of sublethal concentrations of DAP (0.5× MIC with 2 μg/ml 50 mg/liter Ca^2), after which the adjusted inoculum was plated onto MH agar containing 0.5× MIC of DAP (2 μg/ml). OXA Etest strips were placed on the plates, and the plates were incubated for 24 h. (C) Western blot (WB) analysis of the PBP 2a present in cell membrane extracts collected from cells as described in the legend to panel A. (D) Quantitation of *mecA* mRNA by real-time RT-PCR using RNA prepared from CB5014 and CB5014IndD. Relative fold changes are shown; 16S rRNA was used as an internal control. # and *, the fold change was significantly greater than that for the control ($P < 0.05$ and $P < 0.01$, respectively). C, control; D, daptomycin; Ox, oxacillin; D/O, daptomycin-oxacillin.

level of β-lactam resistance different from that seen in the heterogeneous MRSA strains (e.g., CB1634) whose cell populations are able to express differential levels of resistance and that are mostly associated with lower MICs (1 to 32 μg/ml).

We hypothesized that the absence of DAP selection prevented detection of the seesaw effect in these strains. We tested this idea by growing cultures of DAP^r strain CB5014 in the presence of a sublethal concentration (0.5× MIC) of DAP (2 μg/ml DAP, 50 mg/liter Ca^{2+}), after which the adjusted inoculum was plated onto Mueller-Hinton (MH) agar containing 0.5× MIC of DAP (2 μg/ml). OXA Etest strips were placed on the plates, and the plates were incubated for 24 h, after which a pronounced decrease in the OXA MIC from 512 μg/ml to 1 μg/ml was observed (Fig. 7A and B); this strain with low-level resistance induced by DAP is referred as CB5014IndD. Similar results were obtained with DAP^r strain CB5036 (data not shown). In support of these observations, PBP 2a was detectable in membrane extracts from CB5014 grown overnight without DAP induction and then exposed to DAP-OXA, whereas under the same conditions, the levels of the protein in CB5014IndD became almost undetectable (Fig. 7C). These results are consistent with the appearance of the DAP-mediated seesaw effect, as it was displayed only in the CB5014IndD strain. Furthermore, as shown above for CB1634 (Fig. 4A), the absence of PBP 2a in cell membrane extracts collected from CB5014IndD was

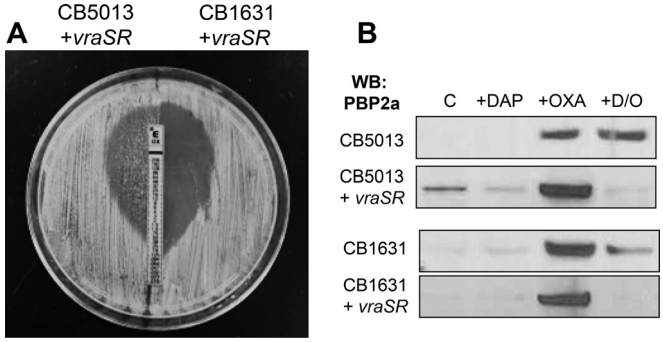

FIG 8 VraSR- and DAP-mediated seesaw effect. (A) CB5013+*vraSR* and CB1631+*vraSR* were grown overnight, after which the adjusted inoculum was plated onto MH agar, OXA Etest strips were placed on the plates, and the plates were incubated at 37°C for 24 h. (B) Western blot analysis of the PBP 2a present in cell membrane extracts collected under the indicated conditions from DAP^s CB5013 and CB1631 and their corresponding *vraSR*-overexpressing counterparts (CB5013+*vraSR* and CB1631+*vraSR*, respectively).

not related to a decrease in the levels of *mecA* mRNA transcription: in the presence of OXA, either alone or in combination with DAP, *mecA* expression was highly induced (~4- and 5.6-fold, respectively; Fig. 7D). CB5014 exposed to OXA or OXA-DAP also showed increased levels of *mecA* expression, although the level of expression was lower than that observed in CB5014IndD (Fig. 7D). Together, these data suggest that homogeneous DAP^r MRSA strains rely upon DAP induction-mediated factors to express the seesaw phenotype.

Role of VraSR in the DAP-mediated seesaw effect. As mentioned above, we previously demonstrated the critical role played by the VraSR two-component regulatory system in the acquisition of DAP^r (20) Moreover, DAP^r strains, including the CB5014 and CB5035 homogeneous MRSA strains, expressed higher levels of *vraSR* than their corresponding DAP^s counterparts (20). To further elucidate and understand the mechanistic role of DAP-induced *vraSR* expression and the seesaw effect, we overexpressed *vraSR* in the corresponding DAP^s CB5013 (OXA MIC, 512 μg/ml) and CB1631 (OXA MIC, 32 μg/ml) strains. This resulted in *vraSR* expression levels similar to those observed in the corresponding DAP^r counterparts, CB5014 and CB1634, as determined by RT-PCR (data not shown). Phenotypic analyses performed by the OXA Etest showed that CB5013 overexpressing *vraSR* (strain CB5013+*vraSR*) and CB1631 overexpressing *vraSR* (strain CB1631+*vraSR*) displayed both DAP-mediated seesaw effects, i.e., decreased DAP susceptibility (DAP MICs, 4 μg/ml) and oxacillin resistance (OXA MICs, 0.25 and 0.5 μg/ml for DAP^s CB5013+*vraSR* and CB1631+*vraSR*, respectively; Fig. 8A). Moreover, analysis of the *mprF* DNA sequences in these strains revealed amino acid changes that were identical to those present in their DAP^r counterparts (S337L in CB5014 and L826F in CB1634), demonstrating that the increased expression of *vraSR* mediated by DAP leads to polymorphisms in *mprF*. To investigate further the potential role of increased *vraSR* expression mediated by DAP in changes in antibiotic susceptibilities related to the seesaw effect, we analyzed the PBP 2a levels in cell membrane lysates from strains CB5013 and CB1631+*vraSR*. As depicted in Fig. 8B, increased PBP 2a levels were observed at the baseline in CB5013+*vraSR* compared to those observed in the other strains. When all strains were exposed to OXA alone, they showed increased amounts of cell membrane-associated PBP 2a. Importantly however, membrane-associated PBP 2a was undetectable following exposure to DAP-OXA in both strains expressing higher levels of *vraSR*, consistent with the seesaw effect described above.

To gain further insights into potential differences between the strains displaying the seesaw effect, i.e., CB1634 and CB5014IndD, we compared the overall gene expression profiles of the strains by comparing RNA-Seq data after exposure to OXA or DAP-OXA. Expression of approximately 322 genes was significantly altered (determined by a *P* value of <0.05 and a more than 2-fold difference in the level of expression before and

after exposure to OXA or DAP-OXA; see Table S1 in the supplemental material). Among these genes, relevant observations obtained when the gene expression of CB5014IndD and CB1634 was compared after exposure to DAP-OXA included the upregulation of *vraSR* mRNA (~6-fold), accompanied by increased levels of expression of transcripts for the *vraSR* target genes *pbp2* (~4-fold) and *sgtB* (~3.5-fold). In addition, *mecA* mRNA was also highly upregulated (~21- and 5-fold in strains exposed to DAP-OXA and OXA, respectively), as were mRNAs for *mecI* and *mecRI* (~5- and 3-fold). Other genes that were upregulated included those coding for proteins involved in the synthesis of peptidoglycan precursors (*murA* to *murG*, *femAB*, and *mraW*, the levels of expression of which were increased between 6- and 3.9-fold), while downregulated genes were associated with other gene class families, i.e., genes involved in biosynthesis and metabolic pathways, such as those for iron (*fer*, *fmhA*), histidine (*hisG*, *hisH*), and gluconate (*gntP*, *gntK*). Together, these results provide strong evidence supporting the key mechanistic role played by the increased expression of *vraSR* following DAP exposure and its implication in the process leading to the acquisition of DAP resistance and the concomitant seesaw effect.

DISCUSSION

DAP targets the bacterial CM, causing rapid membrane depolarization and cell death (2). Decreased susceptibility to DAP in *S. aureus* has been reported to lead to clinical failures in patients with MRSA deep-site infections, such as endocarditis and abscesses (28–30). Previously, we identified two major factors that mutually cooperate in the acquisition of DAP resistance; one is related to the cell membrane (*mprF* mutations), and the second affects cell wall factors (VraSR) (6). Moreover, we observed that the DAP^r phenotype was accompanied by increased susceptibility to OXA, the so-called seesaw effect. Previously, a concomitant rise in the level of vancomycin resistance with decreased β-lactam resistance has been reported in some clinical vancomycin-intermediate *S. aureus* (VISA) and vancomycin-resistant *S. aureus* (VRSA) strains. In VISA strains, the mechanism remains undefined, with some strains showing excision of SCC*mec* carrying *mecA*, while in others *mecA* is retained (31, 32). In contrast, in VRSA strains, the loss of β-lactam resistance seems to be associated with the inability of PBP 2a to utilize the UDP-*N*-acetylmuramic acid-depsipeptide (D-Ala–D-Lac) cell wall precursor produced in VRSA for transpeptidation, leaving PBP 2 to be essential for the synthesis of the abnormally structured cell wall (33). To date, the precise mechanism responsible for the seesaw effect mediated by DAP resistance in MRSA still remains to be elucidated.

Based on the findings of the present study, we postulate that DAP-induced *mprF* mutations at the CM level cause alterations that affect the localization and functions of important proteins involved in cell wall construction. In this context, it has previously been noted that subinhibitory concentrations of DAP induce aberrant and asymmetric division septa in *B. subtilis* (20), reinforcing the notion that DAP may target both the CM and CW. Working on the hypothesis that, by targeting the CM, DAP perturbs the lipid environment of membrane-bound enzymes involved in peptidoglycan synthesis, moderately disrupting CW assembly, we found that exposure of DAP^r cells to a combination of DAP and β-lactams led to the delocalization of peptidoglycan synthesis from the division septum, redistributing this activity around the cell wall. We and others have observed that the seesaw effect is mainly achieved by β-lactams targeting the PBP 1 and/or PBP 2 protein that localizes at the septum of *S. aureus* and, furthermore, that this effect does not depend on other peptidoglycan synthesis enzymes (34). Recently, it has been demonstrated that peptidoglycan synthesis in *S. aureus* can rely solely on PBP 1 and PBP 2 after seven of the nine peptidoglycan synthesis proteins are removed (34). The observation that only β-lactams targeting PBP 1 or PBP 2 are capable of killing cells during exposure to DAP-OXA supports the idea that perturbations to these proteins are largely sufficient for the MRSA sensitization observed during the seesaw effect.

Importantly, we found that sensitization to β-lactams in DAP^r strains containing mutant *mprF* alleles was associated with decreased levels of cell membrane-associated

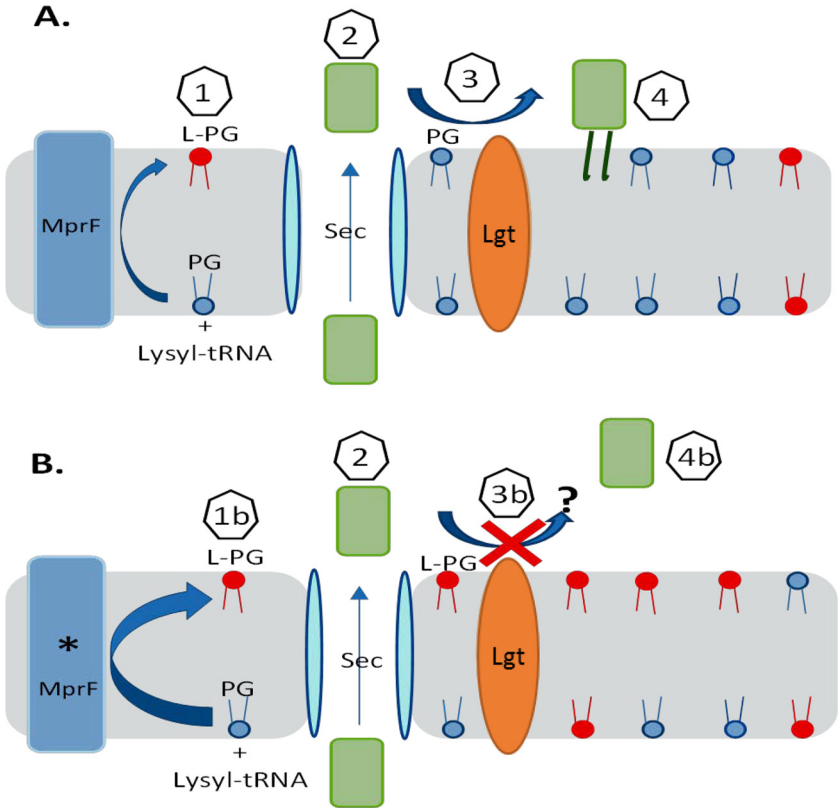

FIG 9 Proposed model of MprF (A) or mutated MprF (* MprF) (B) affecting lipoprotein PrsA anchorage. Step 1, MprF uses cytosolic lysyl-tRNA to convert phosphatidylglycerol (PG) to lysyl phosphatidylglycerol (L-PG); step 1b, the enhanced transferase and/or flippase activity of mutated MprF increases the proportion of L-PG compared to that of phosphatidylglycerol in the outer membrane leaflet; step 2, prelipoprotein PrsA is secreted, which probably occurs through the Sec pathway; step 3, phosphatidylglycerol is used by the Lgt enzyme to lipid modify the PrsA lipobox cysteine; step 3b, inhibition of Lgt-mediated acyl transfer to PrsA occurs due to increased L-PG amounts/reduced phosphatidylglycerol amounts in the outer membrane leaflet; step 4, lipidated membrane-anchored PrsA helps with the posttranslational maturation of PBP 2a; step 4b, failure to produce lipidated membrane-anchored PrsA occurs.

PBP 2a. MprF is involved in the modification of phosphatidylglycerol, which acts as a substrate for Lgt to modify lipoproteins, such as PrsA, with lipid moieties (27). The present evidence highlights potential mutual interactions between MprF and PrsA during DAP^r. In fact, it is plausible to postulate that cell membrane modifications triggered by DAP^r-mediated mutated MprF may affect both PrsA location and chaperone functions, which are required for PBP 2a folding. In support of the importance of posttranscriptional regulation, we observed reduced amounts of cell membrane-associated PBP 2a in DAP-OXA-treated cells, despite the increased transcription of *mecA* through *mec* regulatory elements. These findings are in agreement with recent observations by Jousselin et al. suggesting that PBP 2a is a related substrate of PrsA (13), although we cannot rule out the possibility that PrsA may also influence the septal localization of PBPs, specifically, PBP 1 and PBP 2, which are associated with the seesaw effect and are PrsA substrates in three Gram-positive bacterial pathogens (18).

We have previously established a role for the lipoprotein PrsA as an important mediator of both glycopeptide and oxacillin resistance, with the latter occurring through its effect on the potential proper maturation of PBP 2a (13, 14). A consideration of MprF and the biosynthesis of lipoproteins, such as PrsA, suggests a plausible model to explain the seesaw effect linking DAP nonsusceptibility and decreased resistance to certain antistaphylococcal β-lactams in MRSA strains (Fig. 9).

The integral membrane protein MprF uses cytosolic charged lysyl-tRNA to lysinylate

phosphatidylglycerol and subsequently flips lysyl phosphatidylglycerol (L-PG) to the outer leaflet of the cytoplasmic membrane. Mutated MprF showing enhanced enzymatic transferase and/or flippase activity results in a significantly increased proportion of L-PG in the membrane compared to that of peptidoglycan, as well as the generation of membrane L-PG asymmetry by the selective accumulation of L-PG in the outer leaflet (35, 36).

Prelipoproteins mature sequentially by secretion, lipidation of the lipobox cysteine embedded within the signal sequence by phosphatidylglycerol and Lgt acyltransferase, and finally, signal sequence cleavage by Lsp (37, 38). The study of LgtA in *Escherichia coli* demonstrated that the *S. aureus* enzyme could fully compensate for the *E. coli* enzyme (39). Further high-resolution X-ray structure and function analysis of the *E. coli* enzyme revealed mechanistic features consistent with an active site facing the periplasm and acquisition of the phosphatidylglycerol substrate from the outer membrane leaflet (40). Phosphatidylglycerol is used as a substrate lipid by at least four enzymes, MprF, LtsA, Cls1/2, and Lgt, to control the biosynthesis of L-PG, the polymerization of lipoteichoic acid glycerol phosphate, cardiolipin, and the lipidation of lipoproteins, respectively. Only LtsA is essential, indicating that the activities provided by the other enzymes when phosphatidylglycerol is used as a substrate are facultative (27, 36). Since LtsA governs an essential process mediating the production of lipoteichoic acid, it is reasonable to ask, what permits lipobox lipidation to continue, if at all, in DAP^r strains arising from mutated MprF (or enhanced GraRS activity driving MprF production) as L-PG accumulates and the amount of phosphatidylglycerol diminishes in the outer membrane leaflet?

We hypothesize that disruption of lipoprotein anchorage by inhibition of Lgt-mediated acyl transfer contributes to the seesaw mechanism. Our model predicts that the proper function of PrsA in particular is disrupted, and this is in accordance with our experimental findings. Failure to produce sufficient lipidated PrsA would impair PrsA-dependent posttranslational maturation of PBP 2a, allowing transpeptidase activity to be susceptible to β-lactams. Of course, we cannot exclude the possibility of the existence of alternative scenarios in which other lipoproteins, such as DsbA, could affect protein function (41) or in which the membrane electrostatic charge has effects on membrane-associated sensory processes that regulate cell wall biosynthesis (26). In support of the specific role of PrsA, we have produced a PrsA lipobox cysteine mutant that we could not detect in membrane extracts by Western blot analysis, suggesting that it is unstable and degraded or fails to anchor and is lost (A. Jousselin and A. Renzoni, unpublished data).

The intriguing observation that some DAP^r strains do not display a seesaw effect unless they are preinduced with sublethal levels of DAP prompted us to investigate in more detail the role of VraSR. Indeed, we found that overproduction of VraSR in DAP^s strains decreased susceptibility to DAP and increased susceptibility to β-lactams, similar to the findings obtained with LiaFSR, a pivotal regulator of DAP^r in enterococci (42). In the absence of DAP, the three-component regulatory system LiaFSR is turned off by the negative interaction of LiaF with LiaS. LiaS responds to membrane stress by phosphorylating LiaR, which leads to changes in the levels of transcription of several downstream operons that affect CM homeostasis (42). Interestingly, in enterococci the ability of several β-lactams, especially ampicillin (AMP), ceftaroline (CPT), and ertapenem (ERT), to provide synergistic activity with DAP and prevent the emergence of DAP nonsusceptibility has also been demonstrated (43, 44).

In *S. aureus*, VraS belongs to a subfamily of kinases that sense cell envelope stress and do not contain extracellular sensor domains (45). Although the transmembrane helices of this subgroup have been proposed to be involved in stress sensing, the precise mechanism of VraS-like kinase activation remains unknown. We propose that exposure of DAP^r strains to DAP-OXA determines the reorganization of the membrane structure through the induction of changes in phospholipid composition which may activate VraSR signaling by promoting VraS dimerization and downstream events, including autophosphorylation of VraS, phosphorylation of VraR, and gene regulation.

TABLE 2 Strains and primers used in this study

Strain or primer	Description or sequence	Reference or source
S. aureus strains		
CB5011	Daptomycin susceptible	6
CB5012	Daptomycin-resistant strain isogenic to CB5011, *mprFL826F*	6
CB5013	Daptomycin susceptible	6
CB5014	Daptomycin-resistant strain isogenic to CB5013, *mprFS377L*	6
CB1631	Daptomycin susceptible	6
CB1634	Daptomycin-resistant strain isogenic to CB1631, *mprFL826F*	6
MAR17	CB1634 Δ*mprF*::*cat*	6
MAR18	MAR-17/pMPRF-1 (wild type)	6
MAR19	MAR-17/pMPRF-2 (L826F mutant)	6
CB5013+VraSR	Entire *vraS* and *vraR* sequences cloned into pAW8	This study; 49
CB1631+VraSR	*vraS* and *vraR* sequences cloned into pAW8	
Primers and probes		
PrsA-F	AGTTAATGATAAGAAGATTGACGA	
PrsA-R	GAAGGGCCTTTTCAAATTTATCTTT	
VraSR-F	GGTGCAACGTTCCCATATTGTATTGT	
VraSR-R	GGCTTCAACTCATGGGCTTTGGCAA	
mprF-F	GGTGGCTTTATTGGTGCAGGCG	
mprF-R	GATGCATCGAAAACATGGAA	
mecA-F	TGCCTAATCTCATTGTGTTCCTGTAT	
mecA-R	CGGTGCTGAAACTTTCACAATATAAT	
pbp2-GFPF (DPH407)	GATAGCGGCCGCATGACGGAAAACAAAGGATCTTCTC	
pbp2-GFPR (DPH408)	GAAGGGATCCTTAGTTGAATATACCTGTTAATCCACCG	
16S-F	TCCGGAATTATTGGGCGTAA	
16S-R	CCACTTTCCTCTTCTGCACTCA	

Based on our observations, we postulate that the induction of changes by DAP, such as those seen in the CB5014IndD strain, may favor the oligomerization of VraR, which in turn may form a constitutively activated tetramer with a high affinity for DNA, even in the absence of phosphorylation, favoring the development of DAP resistance and the seesaw effect phenotype, as in heterogeneous DAP^r MRSA strain CB1634. We are currently studying the differences in VraR oligomerization among DAP^r clinical strains that may explain the differences between heterogeneous and homogeneous DAP^r MRSA strains.

In summary, the present study addresses the mechanistic bases and significance of sensitization to β-lactams linked to DAP^r in clinical MRSA strains. The combination of DAP and β-lactams has gained increased acceptance for the treatment of MRSA infections produced by DAP^r strains, resulting in clinical successes. We demonstrate that VraSR is a key determinant of DAP resistance, leading to mutations in *mprF* that may impair PrsA chaperone functions, which are required for the posttranscriptional maturation of PBP 2a; these effects may account for the resensitization of DAP^r strains to cell wall-specific β-lactams. Continued progress in understanding DAP's mode of action and its impact on the CM/CW machinery will provide fundamental insights into MRSA biology that may potentially be translated into the discovery of new therapeutic targets.

MATERIALS AND METHODS

Bacterial strains and antibiotics. All clinical strains used in this study are listed in Table 2. Trypticase soy agar with 5% sheep blood (BBL, Sparks, MD) was used for the subculture and maintenance of *S. aureus*. *Staphylococcus aureus* and *E. coli* were grown in Mueller-Hinton broth (MHB). Standard reference antibiotics, tetracycline (TET; 3 μg/ml), chloramphenicol (CM; 10 μg/ml), and oxacillin (OXA; concentration range, 0.5 to 10 μg/ml) were obtained from Sigma, St. Louis, MO, or United States Biochemicals, Cleveland, OH. Daptomycin (DAP) was provided by Cubist Pharmaceuticals/Merck (Lexington, MA). DAP and OXA were used at concentrations adjusted on the basis of the MICs for the parental strains and genetic mutants. Calcium was added at a concentration of 50 mg/liter for DAP. Antimicrobial susceptibility to OXA was determined according to the guidelines of the Clinical and Laboratory Standards Institute (46). DAP MICs were determined by Etest (AB Biodisk, Solna, Sweden).

Membrane protein extraction. For the isolation of membrane proteins, strains were grown in MHB until mid-exponential phase, and pellets were resuspended in 600 μl of phosphate-buffered saline (PBS). Bacterial cells were disrupted by adding glass beads and using a FastPrep cell disrupter (MP Biomedicals,

Santa Ana, CA), and the lysate was centrifuged at 8,000 × *g* for 10 min at 4°C. The supernatant fraction was centrifuged for an additional 5 min at 8,000 × *g* at 4°C to remove the beads, and then the supernatant was transferred to ultracentrifuge tubes and centrifuged at 45,000 rpm in a Thermo Sorvall WX Ultra series WX80 centrifuge (Thermo Scientific, Waltham, MA) for 1 h at 4°C. The membrane pellet was resuspended in PBS, and total membrane proteins were quantified by the Bradford protein assay (Thermo Fisher) and stored at −80°C.

Secreted protein preparation. Bacteria were grown in MHB until the OD_{600} was approximately 0.3. Then, the samples were centrifuged for 10 min at 4,000 rpm and the supernatant was passed through 0.22-μm-pore-size membrane filters (Millex). Samples were normalized by adjustment of the volume to equal the sample OD, and 20 μg of carbonic anhydrase (Sigma) was added as an internal spike control as described previously (14). Samples were concentrated in Amicon 10,000-molecular-weight-cutoff centrifugal filters (Millipore) to a final volume of 40 μl.

Western blotting. Proteins (15 μg) were separated on 4 to 12% bis-Tris gels and blot transferred onto pure nitrocellulose blotting membranes (Pall Life Science). The membranes were blocked using 5% low-fat milk in PBS. PBP 2a was probed with monoclonal anti-PBP 2a antibody (Slidex MRSA detection kit; bioMérieux, France) at a 1/2,000 dilution, followed by incubation with a secondary alkaline phosphatase-labeled goat anti-rabbit IgG(H+L) antibody at a 1/5,000 dilution. The labeled protein signal was detected using an SRX/101A film processor (Konica Minolta).

DNA manipulation and sequencing. Chromosomal DNA was prepared by using a Qiagen genomic DNA preparation kit (Qiagen, Inc., Valencia, CA) according to the manufacturer's directions. Sequencing of all PCR amplification products was performed at the Nucleic Acid Research Facility at Genewiz (South Plainfield, NJ). Analysis of the *mprF* sequence in wild-type strains and mutants was performed by using *mprF*-specific primers as previously described (6). Consensus sequences were assembled from both orientations with Lasergene (v12) software (DNAStar, Madison, WI). The *S. aureus* N315 sequence (GenBank accession number BA000018) was used as a reference control.

RNA extraction and RNA-Seq. Total RNA was extracted using an RNeasy isolation kit (Qiagen). The concentration and integrity of the RNA samples were assessed by A_{260}/A_{280} spectrophotometry and gel electrophoresis. RNA samples were cleaned and treated with DNase following the manufacturer's recommendations to avoid potential DNA contamination. RNA was prepared from CB1634 cells collected at exponential phase of growth under the different conditions in the absence and presence of DAP, OXA, and DAP-OXA. The genome-wide transcript sequencing libraries were prepared according to the manufacturer's instructions (ScriptSeq; EpiCenter) and sequenced on a MiSeq instrument (Illumina). Differential gene expression was determined by CLC Genomic Workbench and Lasergene software; differences consisting of >1.5-fold differences in the levels of expression with a P value of <0.05 after application of the Bonferroni correction for multiple comparisons were considered significant.

Analysis of gene expression by RT-PCR. Real-time reverse transcription-PCR (RT-PCR) analysis for RNA samples was done using a SensiMix SYBR one-step kit (Qantace/Bioline, Taunton, MA) according to the manufacturer's protocol. The level of gene expression compared with that for a sample considered the reference (value = 1) was determined using $\log_2-(\Delta\Delta C_T)$, where C_T represents the threshold cycle value. The change (*n*-fold) in the transcript level (ΔC_T) was calculated using the following equations: $\Delta C_T = C_T$ for test DNA – C_T for reference cDNA, $\Delta\Delta C_T = \Delta C_T$ for the target gene − ΔC_T for 16S rRNA, and amount of target = $2^{-\Delta\Delta CT}$. The quantity of cDNA for each experimental gene was normalized to the quantity of 16S cDNA in each sample. The oligonucleotide primers used in this study are shown in Table 2.

Microscopy, labeling, and imaging of DAP^s and DAP^r cells. Parental DAP^s strain CB1631 and resistant DAP^r strain CB1634 were grown to exponential phase in tryptic soy broth (TSB) in the absence and presence of DAP (0.25 and 1 μg/ml, respectively) at 37°C and labeled for 5 min with either HADA (which stains nascent peptidoglycan insertion), FM1-43FX (which stains the cell membrane), DAPI (which stains DNA), or vancomycin (which stains nascent D-alanyl–D-alanine incorporation into the CW) (Sigma) mixed with a Bodipy FL conjugate of vancomycin (VAN-Bodipy FL; Molecular Probes) to a final concentration of 0.8 μg/ml. Images were obtained with a Nikon inverted epifluorescence microscope. For studies on the localization of PBP 2, the corresponding gene, *pbpB*, was expressed as an N-terminal GFP fusion protein in CB1634. Genomic DNA was PCR amplified using Phusion DNA polymerase and primers pbp2-GFPF (DPH407) and pbp2-GFPR (DPH408) (Table 2). PCR fragments were digested with NotI and BamHI and ligated into a cleaved pEA18 vector in frame with *gfp* (originally cloned from pDSW207) to generate pDH177 in *E. coli* AG111 competent cells. The *gfp-pbpB* fragment, including the *B. subtilis spoVG* ribosome binding site sequence of pEA18, was subcloned from pDH177 by digestion with HindIII and BamHI and ligated into the cleaved pCL15 vector to generate pDH178. pDH178 was initially cloned into *E. coli* AG1111 (Promega Wizard) and transformed into *S. aureus* RN4220 by electroporation. The plasmid was then transduced from RN4220 into *S. aureus* CB1634 using phage 80α. CB1634 cells containing the *gfp-pbpB* gene in pDH178 were induced with IPTG in the presence of OXA, DAP, or DAP-OXA to localize PBP 2a during DAP-OXA synergistic effects. Cells were fixed in 2.8% formaldehyde (FA) and 0.04% glutaraldehyde (GA) in growth medium for 15 min at room temperature. The cells were collected by centrifugation at 8,000 × *g* for 5 min, washed once in PBS, treated with Vectashield antifade reagent, and visualized by fluorescence microscopy with an Olympus BX60 epifluorescence microscope containing a ×100 oil immersion objective (numerical aperture, 1.4). Images were captured with a Hamamatsu Orca charge-coupled device camera using HCImage software.

Labeling of PBPs with Bocillin FL. Bocillin FL labeling of 100 μg of membrane proteins was performed with 100 μM Bocillin FL (Molecular Probes), with which the proteins were incubated for 30 min at 35°C. The reaction was stopped by adding 4× SDS-PAGE sample buffer. The labeled membrane

protein concentrations were determined by the Bradford protein assay, 15 μg was loaded on a 10% bis-Tris gel, and the proteins were detected using a ProteinSimple imager-FluorChem E system (GE Healthcare).

Peptidoglycan purification and analysis. Exponentially growing cells (OD_{600}, 0.5) grown on MHB untreated and treated with OXA, DAP, and DAP-OXA were boiled in 4% SDS, deproteinized by treatment with pronase and trypsin, treated with 48% hydrofluoric acid (HF) at 4°C for 16 h, and washed several times with 0.25 M Tris-HCl and water before lyophilization. Purified peptidoglycan was digested with 25 μg/ml of mutanolysin (Sigma). The soluble muropeptides were reduced with sodium borohydride. The reaction was stopped by the addition of phosphoric acid, and the supernatant containing peptidoglycan was analyzed in an LC-20AB HPLC equipped with an SPD-20A UV detector (Shimadzu). The separation of muropeptides was performed in a Jupiter Proteo column (C_{18}, 250 by 4.6 mm, 4 μm, 90 Å; Phenomenex). Twenty microliters of sample was eluted at 0.5 ml/min for 5 min with 95% mobile phase A (100 mM sodium phosphate buffer, pH 3.0, containing 0.00025% sodium azide) and 5% mobile phase B (methanol), and then the proportion of mobile phase B was increased up to 30% at 120 min, as previously described (47). Detection was performed at 206 nm, and peaks were identified by comparison with the elution profile for peptidoglycan from the COL strain, as previously reported (48).

Statistical analyses. Statistical tests were performed using SPSS (v17.0) software for Windows (SPSS Inc., Chicago, IL, USA). The survival data were plotted using the Kaplan-Meier method.

SUPPLEMENTAL MATERIAL

Supplemental material for this article may be found at https://doi.org/10.1128/AAC.01634-16.

TEXT S1, XLS file, 0.1 MB.

ACKNOWLEDGMENTS

We acknowledge Liliana Paz and Regina Fernandez for their contribution to this work.

We have no relevant financial interests to report.

This study was funded in part by Merck (formerly Cubist Pharmaceuticals), Lexington, MA, by NIH grant NIH-R56AI102503-01A1 (principal investigator, A. E. Rosato), and by Swiss National Science Foundation grants 310030-149762 (to A.R.) and 310030-146540 and 310030-166611 (to W.L.K.).

REFERENCES

1. National Nosocomial Infections Surveillance System. 2004. National Nosocomial Infections Surveillance (NNIS) System Report, data summary from January 1992 through June 2004, issued October 2004. Am J Infect Control 32:470–485. https://doi.org/10.1016/j.ajic.2004.10.001.
2. Baltz RH, Miao V, Wrigley SK. 2005. Natural products to drugs: daptomycin and related lipopeptide antibiotics. Nat Prod Rep 22:717–741. https://doi.org/10.1039/b416648p.
3. Arbeit RD, Maki D, Tally FP, Campanaro E, Eisenstein BI. 2004. The safety and efficacy of daptomycin for the treatment of complicated skin and skin-structure infections. Clin Infect Dis 38:1673–1681. https://doi.org/10.1086/420818.
4. Baltz RH. 2009. Daptomycin: mechanisms of action and resistance, and biosynthetic engineering. Curr Opin Chem Biol 13:144–151. https://doi.org/10.1016/j.cbpa.2009.02.031.
5. Bayer AS, Mishra NN, Chen L, Kreiswirth BN, Rubio A, Yang SJ. 2015. Frequency and distribution of single-nucleotide polymorphisms within mprF in methicillin-resistant Staphylococcus aureus clinical isolates and their role in cross-resistance between daptomycin and host defense antimicrobial peptides. Antimicrob Agents Chemother 59:4930–4937. https://doi.org/10.1128/AAC.00970-15.
6. Mehta S, Cuirolo AX, Plata KB, Riosa S, Silverman JA, Rubio A, Rosato RR, Rosato AE. 2012. VraSR two-component regulatory system contributes to *mprF*-mediated decreased susceptibility to daptomycin in *in vivo*-selected clinical strains of methicillin-resistant Staphylococcus aureus. Antimicrob Agents Chemother 56:92–102. https://doi.org/10.1128/AAC.00432-10.
7. Friedman L, Alder JD, Silverman JA. 2006. Genetic changes that correlate with reduced susceptibility to daptomycin in Staphylococcus aureus. Antimicrob Agents Chemother 50:2137–2145. https://doi.org/10.1128/AAC.00039-06.
8. Mehta S, Singh C, Plata KB, Chanda PK, Paul A, Riosa S, Rosato RR, Rosato AE. 2012. β-Lactams increase the antibacterial activity of daptomycin against clinical methicillin-resistant Staphylococcus aureus strains and prevent selection of daptomycin-resistant derivatives. Antimicrob Agents Chemother 56:6192–6200. https://doi.org/10.1128/AAC.01525-12.
9. Rand KH, Houck HJ. 2004. Synergy of daptomycin with oxacillin and other beta-lactams against methicillin-resistant Staphylococcus aureus. Antimicrob Agents Chemother 48:2871–2875. https://doi.org/10.1128/AAC.48.8.2871-2875.2004.
10. Yang SJ, Xiong YQ, Boyle-Vavra S, Daum R, Jones T, Bayer AS. 2010. Daptomycin-oxacillin combinations in treatment of experimental endocarditis caused by daptomycin-nonsusceptible strains of methicillin-resistant Staphylococcus aureus with evolving oxacillin susceptibility (the "seesaw effect"). Antimicrob Agents Chemother 54:3161–3169. https://doi.org/10.1128/AAC.00487-10.
11. Dhand A, Bayer AS, Pogliano J, Yang SJ, Bolaris M, Nizet V, Wang G, Sakoulas G. 2011. Use of antistaphylococcal beta-lactams to increase daptomycin activity in eradicating persistent bacteremia due to methicillin-resistant Staphylococcus aureus: role of enhanced daptomycin binding. Clin Infect Dis 53:158–163. https://doi.org/10.1093/cid/cir340.
12. Moise PA, Amodio-Groton M, Rashid M, Lamp KC, Hoffman-Roberts HL, Sakoulas G, Yoon MJ, Schweitzer S, Rastogi A. 2013. Multicenter evaluation of the clinical outcomes of daptomycin with and without concomitant beta-lactams in patients with Staphylococcus aureus bacteremia and mild to moderate renal impairment. Antimicrob Agents Chemother 57:1192–1200. https://doi.org/10.1128/AAC.02192-12.
13. Jousselin A, Manzano C, Biette A, Reed P, Pinho M, Rosato A, Kelley WL, Renzoni A. 2015. The Staphylococcus aureus chaperone PrsA is a new auxiliary factor of oxacillin resistance affecting penicillin-binding protein 2A. Antimicrob Agents Chemother 60:1656–1666. https://doi.org/10.1128/AAC.02333-15.
14. Jousselin A, Renzoni A, Andrey DO, Monod A, Lew DP, Kelley WL. 2012. The posttranslocational chaperone lipoprotein PrsA is involved in both glycopeptide and oxacillin resistance in Staphylococcus aureus. Antimi-

crob Agents Chemother 56:3629–3640. https://doi.org/10.1128/AAC.06264-11.
15. Pillai DR, Melano R, Rawte P, Lo S, Tijet N, Fuksa M, Roda N, Farrell DJ, Krajden S. 2009. Klebsiella pneumoniae carbapenemase, Canada. Emerg Infect Dis 15:827–829. https://doi.org/10.3201/eid1505.081536.
16. Samra Z, Ofir O, Lishtzinsky Y, Madar-Shapiro L, Bishara J. 2007. Outbreak of carbapenem-resistant Klebsiella pneumoniae producing KPC-3 in a tertiary medical centre in Israel. Int J Antimicrob Agents 30:525–529. https://doi.org/10.1016/j.ijantimicag.2007.07.024.
17. Bowker KE, Holt HA, Lewis RJ, Reeves DS, MacGowan AP. 1998. Comparative pharmacodynamics of meropenem using an in-vitro model to simulate once, twice and three times daily dosing in humans. J Antimicrob Chemother 42:461–467. https://doi.org/10.1093/jac/42.4.461.
18. Cahoon LA, Freitag NE. 2014. Listeria monocytogenes virulence factor secretion: don't leave the cell without a chaperone. Front Cell Infect Microbiol 4:13. https://doi.org/10.3389/fcimb.2014.00013.
19. Hachmann AB, Angert ER, Helmann JD. 2009. Genetic analysis of factors affecting susceptibility of Bacillus subtilis to daptomycin. Antimicrob Agents Chemother 53:1598–1609. https://doi.org/10.1128/AAC.01329-08.
20. Pogliano J, Pogliano N, Silverman JA. 2012. Daptomycin-mediated reorganization of membrane architecture causes mislocalization of essential cell division proteins. J Bacteriol 194:4494–4504. https://doi.org/10.1128/JB.00011-12.
21. Berti AD, Sakoulas G, Nizet V, Tewhey R, Rose WE. 2013. β-Lactam antibiotics targeting PBP1 selectively enhance daptomycin activity against methicillin-resistant Staphylococcus aureus. Antimicrob Agents Chemother 57:5005–5012. https://doi.org/10.1128/AAC.00594-13.
22. Berti AD, Theisen E, Sauer JD, Nonejuie P, Olson J, Pogliano J, Sakoulas G, Nizet V, Proctor RA, Rose WE. 2015. Penicillin binding protein 1 is important in the compensatory response of Staphylococcus aureus to daptomycin-induced membrane damage and is a potential target for β-lactam–daptomycin synergy. Antimicrob Agents Chemother 60:451–458. https://doi.org/10.1128/AAC.02071-15.
23. Turner RD, Hurd AF, Cadby A, Hobbs JK, Foster SJ. 2013. Cell wall elongation mode in Gram-negative bacteria is determined by peptidoglycan architecture. Nat Commun 4:1496. https://doi.org/10.1038/ncomms2503.
24. Turner RD, Ratcliffe EC, Wheeler R, Golestanian R, Hobbs JK, Foster SJ. 2010. Peptidoglycan architecture can specify division planes in Staphylococcus aureus. Nat Commun 1:26. https://doi.org/10.1038/ncomms1025.
25. Pinho MG, Errington J. 2005. Recruitment of penicillin-binding protein PBP2 to the division site of Staphylococcus aureus is dependent on its transpeptidation substrates. Mol Microbiol 55:799–807. https://doi.org/10.1111/j.1365-2958.2004.04420.x.
26. Hyyrylainen HL, Pietiainen M, Lunden T, Ekman A, Gardemeister M, Murtomaki-Repo S, Antelmann H, Hecker M, Valmu L, Sarvas M, Kontinen VP. 2007. The density of negative charge in the cell wall influences two-component signal transduction in Bacillus subtilis. Microbiology 153:2126–2136. https://doi.org/10.1099/mic.0.2007/008680-0.
27. Stoll H, Dengjel J, Nerz C, Gotz F. 2005. Staphylococcus aureus deficient in lipidation of prelipoproteins is attenuated in growth and immune activation. Infect Immun 73:2411–2423. https://doi.org/10.1128/IAI.73.4.2411-2423.2005.
28. Dubrac S, Boneca IG, Poupel O, Msadek T. 2007. New insights into the WalK/WalR (YycG/YycF) essential signal transduction pathway reveal a major role in controlling cell wall metabolism and biofilm formation in Staphylococcus aureus. J Bacteriol 189:8257–8269. https://doi.org/10.1128/JB.00645-07.
29. Julian K, Kosowska-Shick K, Whitener C, Roos M, Labischinski H, Rubio A, Parent L, Ednie L, Koeth L, Bogdanovich T, Appelbaum PC. 2007. Characterization of a daptomycin-nonsusceptible vancomycin-intermediate Staphylococcus aureus strain in a patient with endocarditis. Antimicrob Agents Chemother 51:3445–3448. https://doi.org/10.1128/AAC.00559-07.
30. Mangili A, Bica I, Snydman DR, Hamer DH. 2005. Daptomycin-resistant, methicillin-resistant Staphylococcus aureus bacteremia. Clin Infect Dis 40:1058–1060. https://doi.org/10.1086/428616.
31. Sieradzki K, Leski T, Dick J, Borio L, Tomasz A. 2003. Evolution of a vancomycin-intermediate Staphylococcus aureus strain in vivo: multiple changes in the antibiotic resistance phenotypes of a single lineage of methicillin-resistant S. aureus under the impact of antibiotics administered for chemotherapy. J Clin Microbiol 41:1687–1693. https://doi.org/10.1128/JCM.41.4.1687-1693.2003.
32. Sieradzki K, Tomasz A. 1999. Gradual alterations in cell wall structure and metabolism in vancomycin-resistant mutants of Staphylococcus aureus. J Bacteriol 181:7566–7570.
33. Severin A, Wu SW, Tabei K, Tomasz A. 2004. Penicillin-binding protein 2 is essential for expression of high-level vancomycin resistance and cell wall synthesis in vancomycin-resistant Staphylococcus aureus carrying the enterococcal vanA gene complex. Antimicrob Agents Chemother 48:4566–4573. https://doi.org/10.1128/AAC.48.12.4566-4573.2004.
34. Reed P, Atilano ML, Alves R, Hoiczyk E, Sher X, Reichmann NT, Pereira PM, Roemer T, Filipe SR, Pereira-Leal JB, Ligoxygakis P, Pinho MG. 2015. Staphylococcus aureus survives with a minimal peptidoglycan synthesis machine but sacrifices virulence and antibiotic resistance. PLoS Pathog 11:e1004891. https://doi.org/10.1371/journal.ppat.1004891.
35. Bayer AS, Schneider T, Sahl HG. 2013. Mechanisms of daptomycin resistance in Staphylococcus aureus: role of the cell membrane and cell wall. Ann N Y Acad Sci 1277:139–158. https://doi.org/10.1111/j.1749-6632.2012.06819.x.
36. Kuhn S, Slavetinsky CJ, Peschel A. 2015. Synthesis and function of phospholipids in Staphylococcus aureus. Int J Med Microbiol 305:196–202. https://doi.org/10.1016/j.ijmm.2014.12.016.
37. Hutchings MI, Palmer T, Harrington DJ, Sutcliffe IC. 2009. Lipoprotein biogenesis in Gram-positive bacteria: knowing when to hold 'em, knowing when to fold 'em. Trends Microbiol 17:13–21. https://doi.org/10.1016/j.tim.2008.10.001.
38. Sankaran K, Wu HC. 1994. Lipid modification of bacterial prolipoprotein. Transfer of diacylglyceryl moiety from phosphatidylglycerol. J Biol Chem 269:19701–19706.
39. Qi HY, Sankaran K, Gan K, Wu HC. 1995. Structure-function relationship of bacterial prolipoprotein diacylglyceryl transferase: functionally significant conserved regions. J Bacteriol 177:6820–6824.
40. Mao G, Zhao Y, Kang X, Li Z, Zhang Y, Wang X, Sun F, Sankaran K, Zhang XC. 2016. Crystal structure of E. coli lipoprotein diacylglyceryl transferase. Nat Commun 7:10198. https://doi.org/10.1038/ncomms10198.
41. Dumoulin A, Grauschopf U, Bischoff M, Thony-Meyer L, Berger-Bachi B. 2005. Staphylococcus aureus DsbA is a membrane-bound lipoprotein with thiol-disulfide oxidoreductase activity. Arch Microbiol 184:117–128. https://doi.org/10.1007/s00203-005-0024-1.
42. Davlieva M, Shi Y, Leonard PG, Johnson TA, Zianni MR, Arias CA, Ladbury JE, Shamoo Y. 2015. A variable DNA recognition site organization establishes the LiaR-mediated cell envelope stress response of enterococci to daptomycin. Nucleic Acids Res 43:4758–4773. https://doi.org/10.1093/nar/gkv321.
43. Munita JM, Panesso D, Diaz L, Tran TT, Reyes J, Wanger A, Murray BE, Arias CA. 2012. Correlation between mutations in liaFSR of Enterococcus faecium and MIC of daptomycin: revisiting daptomycin breakpoints. Antimicrob Agents Chemother 56:4354–4359. https://doi.org/10.1128/AAC.00509-12.
44. Sakoulas G, Nonejuie P, Nizet V, Pogliano J, Crum-Cianflone N, Haddad F. 2013. Treatment of high-level gentamicin-resistant Enterococcus faecalis endocarditis with daptomycin plus ceftaroline. Antimicrob Agents Chemother 57:4042–4045. https://doi.org/10.1128/AAC.02481-12.
45. Mascher T, Helmann JD, Unden G. 2006. Stimulus perception in bacterial signal-transducing histidine kinases. Microbiol Mol Biol Rev 70:910–938. https://doi.org/10.1128/MMBR.00020-06.
46. Clinical and Laboratory Standards Institute. 2007. Performance standards for antimicrobial disk susceptibility tests, 8th ed. Approved standard M2-A8. Clinical and Laboratory Standards Institute, Wayne, PA.
47. Hebert L, Courtin P, Torelli R, Sanguinetti M, Chapot-Chartier MP, Auffray Y, Benachour A. 2007. Enterococcus faecalis constitutes an unusual bacterial model in lysozyme resistance. Infect Immun 75:5390–5398. https://doi.org/10.1128/IAI.00571-07.
48. de Jonge BL, Chang YS, Gage D, Tomasz A. 1992. Peptidoglycan composition of a highly methicillin-resistant Staphylococcus aureus strain. The role of penicillin binding protein 2A. J Biol Chem 267:11248–11254.
49. Boyle-Vavra S, Yin S, Daum RS. 2006. The VraS/VraR two-component regulatory system required for oxacillin resistance in community-acquired methicillin-resistant Staphylococcus aureus. FEMS Microbiol Lett 262:163–171. https://doi.org/10.1111/j.1574-6968.2006.00384.x.